Progress In Electromagnetics Research, Vol. 138, 293–306, 2013

TRANSMISSION TUNNELING THROUGH THE MULTILAYER DOUBLE-NEGATIVE AND DOUBLE-POSITIVE SLABS

Cumali Sabah[1, *], Haci T. Tastan[2], Furkan Dincer[3], Kemal Delihacioglu[4], Muharrem Karaaslan[3], and Emin Unal[3]

[1]Department of Electrical and Electronics Engineering, Middle East Technical University, Northern Cyprus Campus, Kalkanlı, Guzelyurt, TRNC, Mersin 10, Turkey

[2]ISGUM, Ankara Merkez Laboratuvarı, Istanbul Yolu, 14. Km, Köyler, Ankara 06370, Turkey

[3]Department of Electrical and Electronics Engineering, Mustafa Kemal University, Iskenderun, Hatay 31200, Turkey

[4]Department of Electrical and Electronics Engineering, Kilis 7 Aralik University, Kilis 79000, Turkey

Abstract—Transmission tunneling properties and frequency response of multilayer structure are theoretically presented by using transfer matrix method. The structure is composed of double-negative and double-positive slabs which is sandwiched between two semi-infinite free space regions. Double-negative layers are realized by using Lorenz and Drude medium parameters. The transmission characteristics of the proposed multilayer structure based on the constitutive parameters, dispersion, and loss are analyzed in detail. Finally, the computations of the transmittance for multilayer structure are presented in numerical results. It can be seen from the numerical results that the multilayer structure can be used to design efficient filters and sensors for several frequency regions.

1. INTRODUCTION

Electromagnetic (EM) wave interaction with materials is generally described by the materials' constitutive parameters such as permittivity and permeability. In conventional media, called as double-positive

Received 31 January 2013, Accepted 18 March 2013, Scheduled 25 March 2013

* Corresponding author: Cumali Sabah (sabah@metu.edu.tr).

(DPS) media, the mentioned parameters are positive. Therefore, the electric and magnetic fields, and the direction of propagation of the EM wave obey the right-hand rule. However, double-negative (DNG) media have extraordinary features, notably negative constitutive parameters that make the direction of propagation in the opposite direction with respect to DPS media [1]. In this sense, DNG medium (or left handed material, LHM), can be defined as a medium with simultaneously negative permittivity and permeability over a certain frequency band. Such medium can be constructed artificially to provide a frequency dispersive spectrum of the effective constitutive parameters (Lorentz or Drude models) [2–4]. In the mentioned models, the constitutive parameters can be arranged to be simultaneously negative below the electric and/or magnetic plasma frequency. Accordingly, these models can theoretically be used to designate a metamaterial (MTM) system (including multilayer MTM structure) for creating/realizing new functional devices [4–18]. Additionally, the Lorentz and Drude models as MTMs have been utilized in many studies in which one of them is the multilayer MTM system with the application of EM filters [12]. Different than Ref. [12], the proposed stratified MTM system is used for tunneling the transmitted wave which is one the most fascinating application among the other MTM applications such as antenna pattern shaping, cloaking device, modulators, amplifiers, resonators, superlens, sensors, and so on [1–6]. The nature of the tunneling phenomenon comes from the total internal reflection in the multilayer systems. It takes place when the electromagnetic wave propagates from an electromagnetically dense medium to another medium. When the second medium with adequately large refractive index is substituted after the plain medium, propagating wave is reproduced in the third medium under certain conditions. If a DNG medium is placed into the multilayer system, electromagnetic wave can be tunneled through a much greater distance. The comparison between the conventional and MTM structures based on the length sensitivity and impedance mismatch was discussed by B. Edwarset et al. [9]. Furthermore, polarization independent tunneling according to the phase and impedance matching [10] and broadband tunneling based on the constitutive parameters [11] can be given as sample studies in the framework of the wave tunneling with MTM structure(s). Moreover, there are recently some studies about the characterizations of multilayer MTMs for very high frequencies namely optical and terahertz frequency ranges [19–22]. According to those studies, transmission enhancement, sharp transmission peak, and narrow/wide band response can be obtained with suitable MTM designs. There is a compatible agreement between the results of the present study and literature which will be seen in the

following sections. In addition, some recent studies about MTMs and their applications are also given in the references from [23] to [39]. In this study, EM transmission tunneling is investigated based on the multilayer structure composed of DPS and DNG slabs. The analysis and evaluation are performed via the transfer matrix method which is established by imposing the boundary conditions at the interfaces. Non-dispersive and dispersive situations with lossy and lossless cases are investigated for normal incidence to observe the response of the structure for various cases.

2. THEORETICAL ANALYSIS

The configuration of the structure is shown in Figure 1. This multilayer structure has a single DPS layer sandwiched between two DNG slabs. The wave vector $\mathbf{k}_i$ is normally incident from air to the first interface. The slab thicknesses of each layer are denoted by d_i (1, 2, 3) and are selected equal to each other. In the analysis, $\exp(j\omega t)$ time dependence is assumed and suppressed throughout this work.

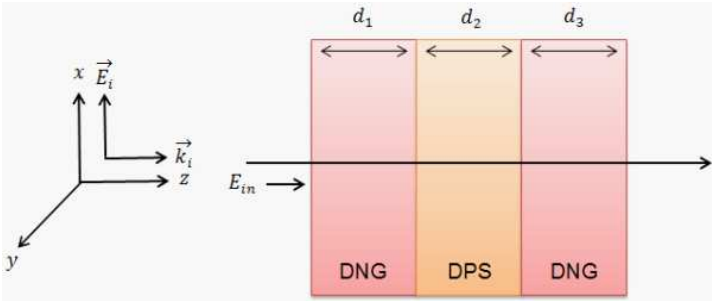

Figure 1. Multilayer structure between two semi-infinite media with the same slab thickness ($d_1 = d_2 = d_3$).

The refractive index and the wave number of DNG slab can be written as:

$$n_{\text{DNG}} = -\sqrt{\varepsilon_{r_{\text{DNG}}} \cdot \mu_{r_{\text{DNG}}}} = -\sqrt{\left(-\varepsilon'_{r_s} + j\varepsilon''_{r_s}\right) \cdot \left(-\mu'_{r_s} + j\mu''_{r_s}\right)}$$
$$= -n'_s + jn''_s \quad (1)$$
$$k_{\text{DNGs}} = k_0 \cdot n_{\text{DNG}} \quad (2)$$

where ε'_{r_s}, ε''_{r_s}, μ'_{r_s}, μ''_{r_s}, n'_s, and n''_s are all real positive numbers. Note that the real part of the complex wave number has to be negative for DNG slab which is a common information known in the literature [15]. The DNG slabs are defined using frequency dispersive Lorenz [12]

and Drude [13] models in which they can provide simultaneously negative permittivity and permeability at a certain frequency band. The permittivity and permeability of a DNG slab can be represented by Drude and Lorentz media parameters as [2–5, 12, 13]:

$$\varepsilon(\omega)=\varepsilon_0\left(1-\frac{\omega_{ep}^2}{\omega^2+j\omega\delta_e}\right)\ \&\ \mu(\omega)=\mu_0\left(1-\frac{F\omega_{mp}^2}{\omega^2-\omega_{m0}^2+j\omega\delta_m}\right) \quad (3)$$

where ω_{ep} is the electric plasma frequency, δ_e the electric damping frequency, ω_{m0} the magnetic resonance frequency, ω_{mp} the magnetic plasma frequency, δ_m the magnetic damping frequency, and F the filling factor. The relationship among the fields in all regions can easily be obtained by using transfer matrix method [40, 41] which is used to obtain reflection and transmission coefficients as:

$$\begin{bmatrix} E_i^+ \\ E_i^- \end{bmatrix} = A \begin{bmatrix} E_{i+2}^+ \\ E_{i+2}^- \end{bmatrix} \quad (4)$$

where A represents the transfer matrix and it can be expressed as;

$$A = \begin{bmatrix} A_{11} & A_{12} \\ A_{21} & A_{22} \end{bmatrix} = \prod_{i=1}^{t+1} P D_i^{-1} D_{i+1} \quad (5)$$

$$D_i = \begin{bmatrix} 1 & 1 \\ 1/Z_i & -1/Z_i \end{bmatrix} \quad (6)$$

$$P = \begin{bmatrix} e^{-i\delta_i} & 0 \\ 0 & e^{-i\delta_i} \end{bmatrix} \quad (7)$$

where D_i^{-1} is inverse matrix of the D_i matrix, δ_i the ith layer phase thickness which can be expressed as $\delta_i = \omega d_i n_i / c$ (c is speed of light in vacuum), Z_i the wave impedance of ith layer, and t the number of slabs. Equation (4) can be extended depending on the layer number. Both the transmission and reflection coefficients can be computed from the matrix A, as given in the following equations.

$$T = \frac{1}{A(1,1)} \quad \& \quad R = \frac{A(2,1)}{A(1,1)} \quad (8)$$

where $A(i, j)$ is the element of the transfer matrix A [40, 41] with $i = 1, 2$ and $j = 1, 2$. Now, the tangential components of the incident, reflected, and transmitted powers which are continuous across the boundaries can be formulated [12]. With the consideration of the energy conservation, the mentioned powers of the system can be given as follows [13–15, 17, 40, 41]:

$$P_{in,z} = \left|\frac{E_{in}^2}{Z_1}\right|; \quad P_{r,z} = \left|\frac{(RE_{in})^2}{Z_1}\right|; \quad P_{t,z} = \left|\frac{(TE_{in})^2}{Z_{t+2}}\right| \quad (9)$$

The energy conservation of the system can be expressed as [13–15, 17, 40, 41]:

$$\left|R^{TE,TM}\right|^2 + \left|\frac{Z_{in,z}}{Z_{t,z}}\right| \cdot \left|T^{TE,TM}\right|^2 = 1 - P_{\text{loss}} \tag{10}$$

3. NUMERICAL RESULTS

In this section, the transmittance as a function of the frequency is demonstrated for various cases to monitor the tunneling phenomenon. To verify the computations, the conservation of power is satisfied for all cases. Then, the transmission line equivalent model as a second method is also obtained for the proposed structure [40, 42]. Both methods give the same results for all computations. Thus, the results are validated by means of two methods. Also, the structure considered in this study consists of three slabs in the form of DNG-DPS-DNG layers. The thicknesses of the slabs are selected as $d_1 = d_2 = d_3 = 1.62\,\text{mm}$. All computations are provided for the normally incident wave. In addition, the semi-infinite media are selected to be free space in all cases.

3.1. Effects of Material Properties in Non-dispersive Lossless Medium

In the first case, the DNG slabs are selected to be identical to each other with the fixed permittivity and permeability as: $\epsilon_{r_{\text{DNG}}} = -0.1$ and $\mu_{r_{\text{DNG}}} = -14$, respectively. The effect of the variation of the permittivity of DPS slab on the transmission is shown in Figure 2. As seen, there is a transmission peak (broad and/or narrow) for different situations. This peak is shifted to higher frequencies and becomes narrower with increasing the permittivity of DPS slab. Higher (lower) permittivity means narrow (broad) band transmission at high (low)

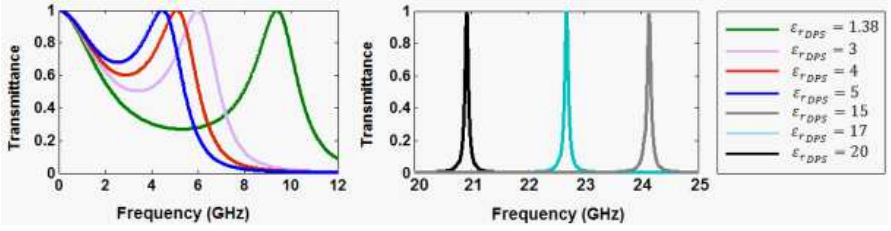

Figure 2. Transmittance as a function of frequency for non-dispersive lossless multilayer structure with fixed DNG parameters ($\epsilon_{r_{\text{DNG}}} = -0.1$, $\mu_{r_{\text{DNG}}} = -14$).

frequency. As a result, the desired spectral location of the transmission peak (correspondingly a reflection dip) with the desired bandwidth can be arranged using the proposed configuration.

As a second investigation, the permeability of the identical DNG slabs are varied when the permittivity of them is selected as $\epsilon_{r_{\mathrm{DNG}}} = -0.1$. Two different cases are considered for the permittivity of DPS slab which are $\epsilon_{r_{\mathrm{DPS}}} = 1.38$ and $\epsilon_{r_{\mathrm{DPS}}} = 15$. According to the results of Figure 3, we have unity or close to unity transmission with broad and narrow bandwidth at the resonant frequency which means a zero and/or minimization in the reflection at the corresponding spectral location. Increasing the permittivity of DPS slab yields a shift in the spectral location of the resonance (transmission peak) to the higher frequencies. In addition, increasing the absolute value of the permeability provides a downshift in the spectral location of the resonance and a narrower transmission peak.

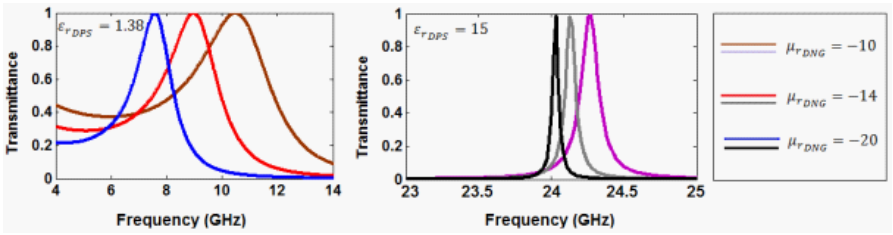

Figure 3. Transmittance as a function of frequency for non-dispersive lossless multilayer structure with fixed DPS parameters (for low and high permittivity cases) and fixed DNG permittivity ($\epsilon_{r_{\mathrm{DNG}}} = -0.1$) when the permeability of DNG medium varied.

In third example, the same configuration is considered expect the constitutive parameters of DNG slabs. The permeability of DNG slabs are fixed to $\mu_{r_{\mathrm{DNG}}} = -14$ and the permittivity is changed. Figure 4 shows the effect of this variation. In the case of the low permittivity of DPS slab, the response of the system is the same as in the previous corresponding case (downshift in the resonance). However, in the case of high permittivity of DPS slab, the structure reveals a focal transmission for the small permittivity of DNG medium at the resonance. The bandwidth can be enhanced by increasing the permittivity of DNG medium. The bandwidth may depend on the impedance matching condition too [16]. In addition, we have two transmission peaks for the broadband configuration when $\epsilon_{r_{\mathrm{DNG}}} = -1$. This can be explained by Fabry Perot system which causes one additional peak [16]. In the high refractive index of DNG slabs, the

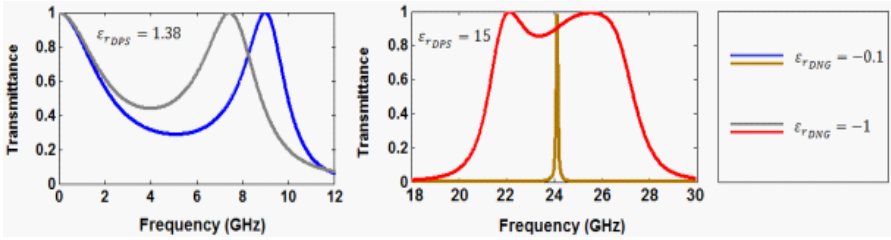

Figure 4. Transmittance as a function of frequency for non-dispersive lossless multilayer structure with fixed DPS parameters (for low and high permittivity cases) and fixed DNG permeability ($\mu_{r_{\mathrm{DNG}}} = -14$) when the permittivity of DNG medium changed.

structure with two reflecting-like surfaces behaves as an effective Fabry Perot medium at high frequencies [16, 40]. As a result, the proposed configuration acts as a narrow and/or broad band-pass EM filter and can be used as an EM sensor owing to its sensitive feature (particularly very narrowband response at high frequency).

3.2. Effects of Loss in Non-dispersive Medium

In this section, the effect of the loss factor will be investigated for non-dispersive medium. In all numerical examples, the effects of high and low loss values on the transmission are investigated for different constitutive parameters. As a first configuration, the permittivity of DPS slab is varied for different loss ratios for two fixed DNG slabs. The results are shown in Figure 5. Increasing the loss factor yields a reduction in the transmission, as known. Upshift and downshift in the spectral location of the resonance are the same with the previous cases.

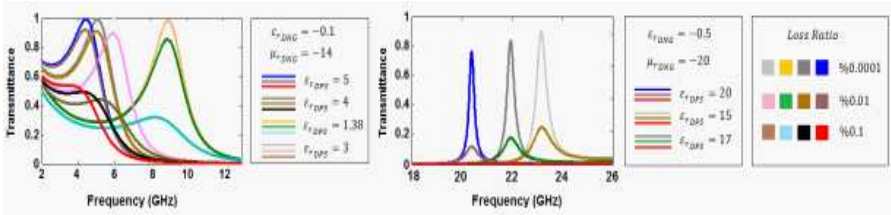

Figure 5. Transmittance as a function of frequency for lossy multilayer structure when the permittivity of DPS slab changed with the fixed DNG parameters (for two cases: $\epsilon_{r_{\mathrm{DNGs}}} = -0.1$, $\mu_{r_{\mathrm{DNGs}}} = -14$ and $\epsilon_{r_{\mathrm{DNGs}}} = -0.5$, $\mu_{r_{\mathrm{DNGs}}} = -20$).

Broadband transmission occurs when DNG slabs have lower refractive index ($\epsilon_{r_{\mathrm{DNGs}}} = -0.1$, $\mu_{r_{\mathrm{DNGs}}} = -14$) while more localized (and very narrow) transmission occurs when DNG slabs have higher refractive index ($\epsilon_{r_{\mathrm{DNGs}}} = -0.5$, $\mu_{r_{\mathrm{DNGs}}} = -20$). The transmission vanishes at the high frequencies when the DNG slabs have higher refractive index. Consequently, the structure can be used for the EM filter and sensor applications [40].

In the following example, the permittivity of DNG slabs is varied when the constitutive parameters of DPS slab and the permeability of DNG slabs ($\mu_{r_{\mathrm{DNG}}} = -14$) are fixed in the presence of the loss. Two different cases are considered for DPS slab ($\epsilon_{r_{\mathrm{DPS}}} = 1.38$ and $\epsilon_{r_{\mathrm{DPS}}} = 15$) and the results are shown in Figure 6. Increasing the loss factor yields the same response as in the previous situation (Upshift/downshift, narrow/broad transmission, and localization). It should be mentioned that the quality of the localization in the transmission with very narrow bandwidth is lost in this configuration compared with the previous arrangements. This means that the structure can be used for EM filter applications.

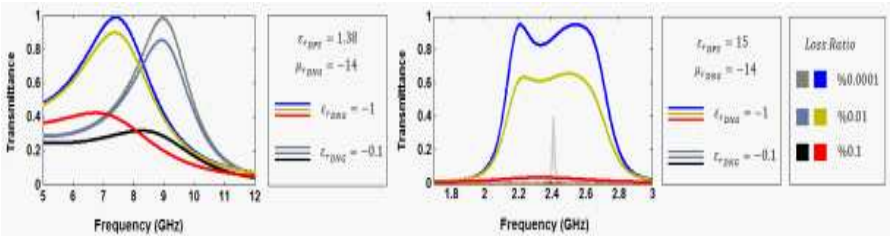

Figure 6. Transmittance as a function of frequency for lossy multilayer structure when the permittivity of DNG slabs is varied with the fixed constitutive parameters of DPS slab and fixed permeability of DNG layers in the presence of the loss.

In the last example of this section, the effect of the permeability on the transmission in the presence of loss is investigated. For this investigation, two different configurations ($\epsilon_{r_{\mathrm{DNG}}} = -0.1$, $\epsilon_{r_{\mathrm{DPS}}} = 1.38$ and $\epsilon_{r_{\mathrm{DNG}}} = -2$, $\epsilon_{r_{\mathrm{DPS}}} = 15$) are considered. Figure 7 shows the results. Increasing the permeability provides an upshift in the resonance (opposite effect of permittivity increase). For high loss, the transmission is minimized or vanished depending on the refractive index of all slabs. No transmission localization is observed. Narrow (not localized and not very narrow) and broadband transmission response is monitored in which the configuration acts as band-pass, low-pass, and high-pass EM filters.

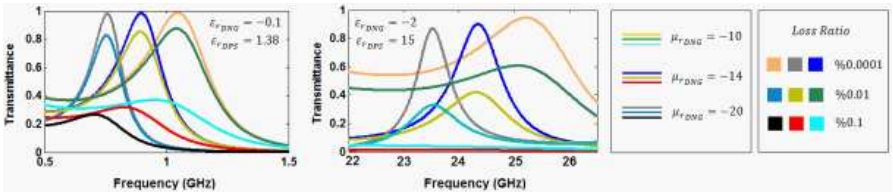

Figure 7. Transmittance as a function of frequency for lossy multilayer structure when the permeability of DNG slabs is varied with the fixed constitutive parameters of DPS slab and fixed permittivity of DNG slabs in the presence of the loss.

3.3. Analysis of the Multilayer Structure for Dispersive Slabs

To establish an accurate and physically realizable system, a multilayer structure with dispersive slabs as DNG media are analyzed by using the Drude and Lorenz parameters. The multilayer structure is investigated for different magnetic and electric plasma frequencies with and without loss (lossless and lossy cases). At first, the magnetic plasma frequency of DNG slabs is varied as shown in Figure 8. There are localization and band-pass characteristics in the transmission. As known, loss reduces the transmission. Increasing the magnetic plasma frequency yields an upshift in the resonance which is directly related with the transmission peak. With the suitable arrangement of the mentioned frequency the spectral location of the resonance can be determined. By proper design of a DNG MTM, this might be possible physically.

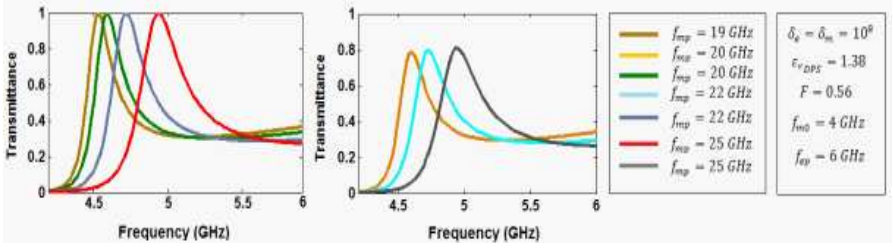

Figure 8. Transmittance as a function of frequency for lossless and lossy dispersive multilayer MTM structure when the magnetic plasma frequency is altered with fixed DPS parameters.

Next, the electric plasma frequency of DNG slabs is changed in the dispersive configuration for lossless and lossy cases. The results are shown in Figure 9. Pass-band characteristic in the transmission is

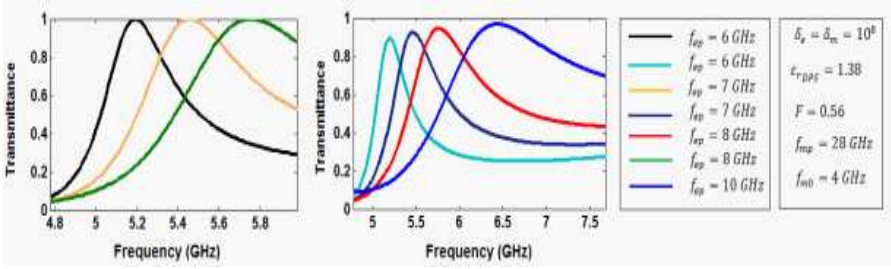

Figure 9. Transmittance as a function of frequency for lossless and lossy dispersive multilayer structure when the electric plasma frequency is altered when the DPS parameters are fixed.

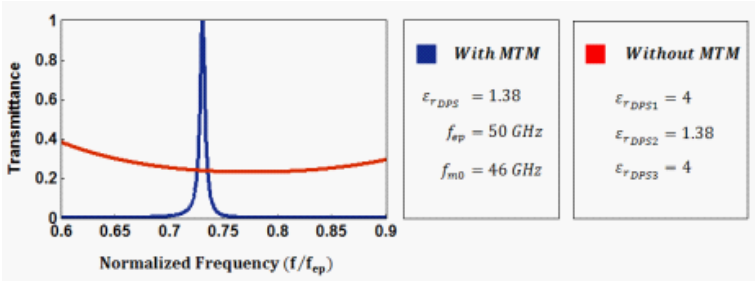

Figure 10. Transmittance as a function of frequency for the multilayer structure with and without DNG layers.

observed. In addition, frequency upshift and enhanced transmission bandwidth properties are monitored. In the presence of loss, the transmission decreases when the electric plasma frequency decreases. More localized transmission might be arranged by using a MTM design having a low electric plasma frequency for EM filtering and particularly sensor applications.

Finally, the transmission spectrum is computed and shown in Figure 10 for proposed three-layer configuration with and without DNG slab for the comparison purpose. The effect of existence of DNG layers in the proposed configuration and corresponding transmission response is analyzed. There are no EM filter and sensor features in the transmission spectra if the configuration has no DNG layer. When DNG layer(s) added to the system, the transmission response can be arranged to be more localized and has a band-gap character. In addition, it can considerably be enhanced with the proper design of DNG slabs of stratified MTM configuration. As a result, the proposed multilayer MTM structure with DNG layer(s) can be utilized as EM filters and sensors.

4. CONCLUSION

A multilayer MTM system is investigated in detail for normally incident plane wave. Transfer matrix method is used for the electromagnetic wave propagation through multilayer MTM structure to obtain the incident, reflected, and transmitted fields. Upshift/downshift in the spectral location of the resonance, band-pass transmission response, narrow/broad band gap character, very sharp transmission peak, and arrangeable EM response are observed from the numerical results. The proposed configurations provide us an opportunity to realize desirable and efficient EM filters and sensors according to the request. In addition, tunable MTM structures can be created based on the obtained results. Besides, the proposed system has multiple degrees of freedom which enable us to easily design and physically realize EM MTM structures. This freedom is provided by the variety of the material parameters mentioned in the previous sections. As a result, multi-functional, flexible, and efficient MTM devices can be created to be used in EM filter and sensor applications for different frequency regimes.

REFERENCES

1. Veselago, V. G., "The electrodynamics of substances with simultaneously negative values of epsilon and mu," *Sov. Phys. Usp.*, Vol. 10, 509–514, 1968.
2. Pendry, J. B., A. Holden, W. Stewart, and I. Youngs, "Extremely low frequency plasmons in metallic mesostructures," *Phys. Rev. Lett.*, Vol. 76, 4773–4776, 1996.
3. Pendry, J. B., A. J. Hollen, D. J. Robbins, and W. J. Stewart, "Magnetism from conductors, and enhanced non-linear phenomena," *IEEE Trans. on Microw. Theory and Tech.*, Vol. 47, 2075–2084, 1999.
4. Shelby, R. A., D. R. Smith, and S. Schultz, "Experimental verification of a negative index of refraction," *Science*, Vol. 292, 77–79, 2001.
5. Fu, C. J., Z. M. Zhang, and D. B. Tanner, "Energy transmission by photon tunneling in multilayer structures including negative index materials," *ASME J. Heat Transf.*, Vol. 127, 1046–1052, 2005.
6. Zhang, Z. M. and C. J. Fu, "Unusual photon tunneling in the presence of a layer with a negative refractive index," *Appl. Phys. Lett.*, Vol. 80, 1097–1099, 2002.

7. Sabah, C. and H. G. Roskos, "Design of a terahertz polarization rotator based on a periodic sequence of chiral-metamaterial and dielectric slabs," *Progress In Electromagnetics Research*, Vol. 124, 301–314, 2012.
8. Sabah, C. and H. G. Roskos, "Broadside-coupled triangular split-ring-resonators for terahertz sensing," *Eur. Phys. J. — Appl. Phys.*, Vol. 61, 30402, 2013.
9. Edwards, B., A. Alu, M. Silveirinha, and N. Engheta, "Comparison between ε-near-zero and fabry-perot resonant transmission through waveguide bends and channels," *XXIX URSI General Assembly*, Chicago, IL, USA, 2008.
10. Luo, Z., Z. Tang, Y. Xiang, H. Luo, and S. Wen, "Polarization-independent low-pass spatial filters based on one-dimensional photonic crystals containing negative-index materials," *Appl. Phys. Lett. B*, Vol. 94, 641–646, 2009.
11. Butler, C. A. M., I. R. Hooper, A. P. Hibbins, J. R. Sambles, and P. A. Hobson, "Metamaterial tunnel barrier gives broadband microwave transmission," *J. Appl. Phys.*, Vol. 109, 013104, 2011.
12. Zhou, X. and G. Hu, "Total transmission condition for photon tunneling in a layered structure with metamaterials," *J. Opt. A: Pure Appl. Opt.*, Vol. 9, 60–65, 2007.
13. Sabah, C. and S. Uckun, "Multilayer system of Lorentz/Drude type metamaterials with dielectric slabs and its application to electromagnetic filters," *Progress In Electromagnetics Research*, Vol. 91, 349–364, 2009.
14. Sabah, C., G. Ogucu, and S. Uckun, "Reflected and transmitted powers of electromagnetic wave through a double-negative slab," *J. Optoelectron. Adv. Mater.*, Vol. 8, 1925–1930, 2006.
15. Sabah, C. and S. Uckun, "Electromagnetic wave propagation through frequency-dispersive and lossy double-negative slab," *Opto.-Electron. Rev.*, Vol. 15, 133–143, 2007.
16. Liu, L., C. Hu, Z. Zhao, and X. Luo, "Multi-passband tunneling effect in multilayered epsilon-near-zero metamaterials," *Opt. Express*, Vol. 17, 12183–12188, 2009.
17. Sabah, C., "Effects of loss factor on plane wave propagation through a left-handed material slab," *Acta Phys. Pol. A*, Vol. 113, 1589–1597, 2008.
18. Ding, Y., Y. Li, H. Jiang, and H. Chen, "Electromagnetic tunneling in nonconjugated epsilon-negative and mu-negative metamaterial pair," *PIERS Online*, Vol. 6, 109–112, 2010.
19. Liu, N., H. C. Guo, L. W. Fu, S. Kaiser, H. Schweizer, and

H. Giessen, "Three-dimensional photonic metamaterials at optical frequencies," *Nature Materials*, Vol. 7, 31–37, 2008.

20. Liu, N., H. Liu, S. Zhu, and H. Giessen, "Stereometamaterials," *Nature Photonics*, Vol. 3, No. 3, 157–162, 2009.
21. Reiten, M. T., D. Roy Chowdhury, J. Zhou, J. F. O'Hara, and A. K. Azad, "Resonance tuning behavior in closely spaced inhomogeneous bilayer metamaterials," *Appl. Phys. Lett.*, Vol. 98, 131105, 2011.
22. Zhou, J., D. R. Chowdhury, R. Zhao, A. K. Azad, H.-T. Chen, C. M. Soukoulis, A. J. Taylor, and J. F. O'Hara, "Terahertz chiral metamaterials with giant and dynamically tunable optical activity," *Physical Review B*, Vol. 86, 035448, 2012.
23. Huang, L. and H. Chen, "Multi-band and polarization insensitive metamaterial absorber," *Progress In Electromagnetics Research*, Vol. 113, 103–110, 2011.
24. Liu, S.-H. and L.-X. Guo, "Negative refraction in an anisotropic metamaterial with a rotation angle between the principal axis and the planar interface," *Progress In Electromagnetics Research*, Vol. 115, 243–257, 2011.
25. Li, J., F.-Q. Yang, and J.-F. Dong, "Design and simulation of L-shaped chiral negative refractive index structure," *Progress In Electromagnetics Research*, Vol. 116, 395–408, 2011.
26. Canto, J. R., C. R. Paiva, and A. M. Barbosa, "Dispersion and losses in surface waveguides containing double negative or chiral metamaterials," *Progress In Electromagnetics Research*, Vol. 116, 409–423, 2011.
27. Giamalaki, M. I. and I. S. Karanasiou, "Enhancement of a microwave radiometry imaging system's performance using left handed materials," *Progress In Electromagnetics Research*, Vol. 117, 253–265, 2011.
28. Xu, S., L. Yang, L. Huang, and H. Chen, "Experimental measurement method to determine the permittivity of extra thin materials using resonant metamaterials," *Progress In Electromagnetics Research*, Vol. 120, 327–337, 2011.
29. Duan, Z., Y. Wang, X. Mao, W.-X. Wang, and M. Chen, "Experimental demonstration of double-negative metamaterials partially filled in a circular waveguide," *Progress In Electromagnetics Research*, Vol. 121, 215–224, 2011.
30. Navarro-Cia, M., V. Torres, M. Beruete, and M. Sorolla, "A slow light fishnet-like absorber in the millimeter-wave range," *Progress In Electromagnetics Research*, Vol. 118, 287–301, 2011.

31. Sabah, C., "Multiband planar metamaterials," *Microwave and Optical Technology Letters*, Vol. 53, 2255–2258, 2011.
32. Cao, T. and M. J. Cryan, "Modeling of optical trapping using double negative index fishnet metamaterials," *Progress In Electromagnetics Research*, Vol. 129, 33–49, 2012.
33. Hasar, U. C., J. J. Barroso, M. Ertugrul, C. Sabah, and B. Cavusoglu, "Application of a useful uncertainty analysis as a metric tool for assessing the performance of electromagnetic properties retrieval methods of bianisotropic metamaterials," *Progress In Electromagnetics Research*, Vol. 128, 365–380, 2012.
34. Hasar, U. C., J. J. Barroso, C. Sabah, and Y. Kaya, "Resolving phase ambiguity in the inverse problem of reflection-only measurement methods," *Progress In Electromagnetics Research*, Vol. 129, 405–420, 2012.
35. Hasar, U. C., J. J. Barroso, C. Sabah, I. Y. Ozbek, Y. Kaya, D. Dal, and T. Aydin, "Retrieval of effective electromagnetic parameters of isotropic metamaterials using reference-plane invariant expressions," *Progress In Electromagnetics Research*, Vol. 132, 425–441, 2012.
36. Sabah, C., "Electric and magnetic excitations in anisotropic broadside-coupled triangular-split-ring resonators," *Appl. Phys. A — Mater. Sci. Process.*, Vol. 108, 457–463, 2012.
37. Sabah, C., "Multi-resonant metamaterial design based on concentric V-shaped magnetic resonators," *Journal of Electromagnetic Waves and Applications*, Vol. 26, Nos. 8–9, 1105–1115, 2012.
38. Sabah, C., "Microwave response of octagon-shaped parallel plates: Low-loss metamaterial," *Optics Communications*, Vol. 285, 4549–4552, 2012.
39. Sabah, C., "Multiband metamaterials based on multiple concentric open ring resonators topology," *IEEE J. Sel. Top. Quantum Electron.*, Vol. 19, 8500808, 2013.
40. Sabah, C., "Analysis, applications, and a novel design of double negative metamaterials," Ph.D. Thesis, Gaziantep University, Gaziantep, Turkey, 2008.
41. Orfanidis, S. J., *Electromagnetic Waves and Antennas*, Rutgers University, online book, 2004.
42. Sabah, C., "Transmission line modeling method for planar boundaries containing positive and negative index media," *IEEE MMET'08 Conference Proceedings*, Odessa, Ukraine, 2008.